JOURNAL OF MATERIALS SCIENCE 20 (1985) 1150–1159

Oxidation resistance and creep behaviour of a silicon nitride ceramic densified with Y_2O_3

A. BOUARROUDJ, P. GOURSAT
Laboratoire des Céramiques Nouvelles, LA CNRS 320, U.E.R. Sciences, 87060 Limoges Cedex, France

J. L. BESSON
Laboratoire des Matériaux Céramiques, LA CNRS 320, E.N.S.C.I., 87065 Limoges Cedex, France

The corrosion resistance and creep behaviour in air of hot-pressed materials with a composition of 70 Si_3N_4–25 SiO_2–5 Y_2O_3 (mol %) has been studied. Kinetics data and microstructural changes in the 1180 to 1650° C temperature range indicate the presence of two oxidation mechanisms. Between 1180 and 1420° C, the preferential oxidation of the intergranular phase containing nitrogen is interpreted in terms of an inward diffusion of ionic oxygen. At temperatures higher than 1420° C, the degradation of the material is the sum of many processes (solution of silicon nitride, migration of oxygen and yttrium and release of nitrogren) but the diffusion to the nitride–oxide interface of a complex combination of yttrium and nitrogen in the boundary phase seems to be the limiting step. The three-point bending creep is discussed in relation to the evolution of the secondary intergranular phases in an oxidizing environment. The creep deformation is the sum of a viscoelastic component and a diffusional component characterized by the same activation energy (720 kJ mol^{-1}).

1. Introduction

It is now well established that for nitrogen ceramics densified with the aid of a liquid-sintering medium, the oxidation resistance and the high temperature mechanical properties are strongly dependent on the residual secondary phases located at grain boundaries and tripple junctions [1, 2]. Whereas many papers have been devoted to the behaviour of Si_3N_4 densified with magnesia, very few results have been published concerning Si_3N_4 sintered with yttria [3].

It has been shown that oxynitride phases [4, 5] in the Si_3N_4–SiO_2–Y_2O_3 system are very sensitive to oxygen and their oxidation at intermediate temperatures leads to the cracking of the sample. On the other hand, materials within the compatibility triangle Si_3N_4–Si_2N_2O–$Y_2Si_2O_7$ show a good resistance up to 1400° C. The aim of the present study was to investigate the corrosion mechanisms and the microstructural changes of a material located in this domain of composition and with a limited amount of vitreous phase (Si_3N_4–SiO_2–Y_2O_3 = 70–25–5 mol %). Experimental results are correlated to the creep data and serve as a basis for the study of the creep behaviour.

2. Sintering and material characterization

Silicon nitride (Alpha Product), silica (Pierce and Warriner Ltd) and yttria (Rhône Poulenc Chimie Fine) of 99.5, 99.5 99.99% purity are mixed by milling in alcohol for 1 h. The slurry is dried for 24 h at 80° C and the aggregates are crushed by hand. The average grain size determined with a particle size analyser (Micromeritics – Sedigraph 5000) is about 5 μm. The powder compacts are made by

0022–2461/85 $03.00 + .12

TABLE I

Starting products (mol%)		Temperature (° C)	Time (h)	Pressure (MPa)	Porosity (%)	Composition (mol%)		
						Si_3N_4	Si_2N_2O	β-$Si_2Y_2O_7$
Si_3N_4	70							
SiO_2	25	1800	2	20	1	71	27	2
Y_2O_3	5							

cold pressing without an organic binder. Hot pressing is carried out in a graphite die under a nitrogen atmosphere. Specimens are discs of 30 mm diameter and 6 mm thick. The sintering conditions and the approximate composition of samples determined with X-ray patterns are summarized in Table I. After sintering, cubes ($5 \times 5 \times 5\,mm^3$) for oxidation tests and bars ($4 \times 4 \times 25\,mm^3$) for mechanical testing are cut from the discs with a diamond saw. All the faces are carefully polished with diamond pastes.

Mechanical tests were performed in air: three-point bending with a 21 mm span.

The flexural strength was determined on a JJ Instruments testing machine at a cross-head speed of $0.5\,mm\,min^{-1}$. The principle of the creep apparatus is based on a classical dead weight concept with a cantilevered (10:1) loading frame. The high temperature extensometer allows a resolution of about 1 μm on the deformation. The high temperatuee part of the loading device is made of alumina.

3. Oxidation

3.1. Experimental techniques

The kinetics obtained in air under isothermal conditions have a parabolic shape with occasional fluctuations. We observe two oxidation intervals; the first one, between 1180 to 1420° C with a very slight weight gain and the second one for temperatures higher than 1420° C at which the reaction is faster.

X-ray patterns of the oxide film at room temperature reveal the presence of silica (tridymite) and of a small amount of yttrium silicate (β-$Si_2Y_2O_7$) in the first domain. For oxidation over 1420° C, yttrium silicate (β-$Si_2Y_2O_7$), silica (α-cristobalite) are formed together with a vitreous phase, the quantity of which increases as the temperature rises.

Optical microscopy studies of cross-sections previously polished enable us to characterize two oxidation phenomena in the first temperature interval. For tests at temperatures lower than 1450° C, one notices a white oxide film on the surface of samples but also a zone, the colour of which is different from the bulk (Fig. 1a). Macrographs of samples oxidized for varying times and at different temperatures, indicate that the colour change is related to the penetration of oxygen. The front of the reaction shifts from the surface to the interior.

Scanning electron micrographs of the scale show crystallites at 1215° C (Fig. 1b) which grow with temperature and give acicular crystals (Fig. 1c). At 1490° C the surface of the glassy oxide layer becomes rough. Because of the plasticity of the scale, nitrogen release creates an important porosity (Fig. 1d). These microstructural data account for the two oxidation domains.

3.2. Discussion

The isothermal curves suggest a diffusion process at it is checked by plotting the square of the fractional weight gain ($\alpha = \Delta Wt/\Delta W_\infty$) $\alpha^2 = K_D t$ as a function of time (Fig. 2). The parabolic rate constants K_D, determined from the slopes of the straight lines in Fig. 2, presented in the diagram $\log K_D = f(T^{-1})$ (Fig. 3) confirm the presence of two oxidation intervals with the following activation energies of $146 \pm 15\,kJ\,mol^{-1}$ and $680 \pm 80\,kJ\,mol^{-1}$.

3.2.1. 1180 to 1420° C interval

At these temperatures an oxide film is formed on the surface and we have noticed a progressive change in the colour. There are several possible explanations for this second reaction. The hypothesis of crystallization of the intergranular phase containing nitrogen can be rejected since the coulour change commences at the surface. After removing the scale, X-ray patterns of the samples oxidized at different fractional weight gains did not reveal any change in the silicon oxynitride content which may result from a limited oxidation of silicon nitride or from a reaction between silicon nitride and the intergranular silica. So, the microstructural changes

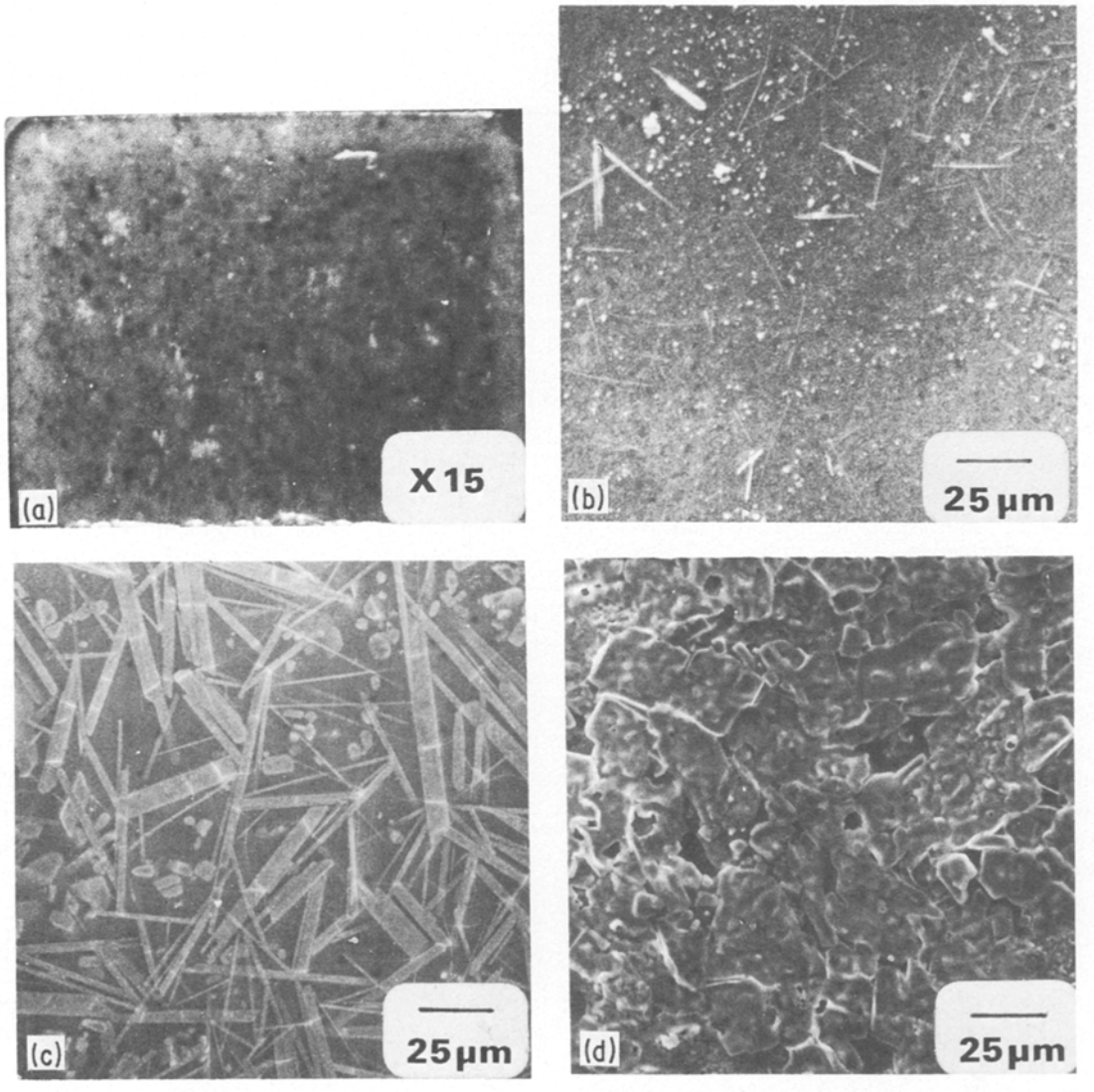

Figure 1 (a) A cross section of a sample oxidized at 1400° C; the greyish zone represents the depth of the oxidation. (b), (c), (d) Scanning electron micrographs of the scale at 1215, 1420 and 1490° C, respectively.

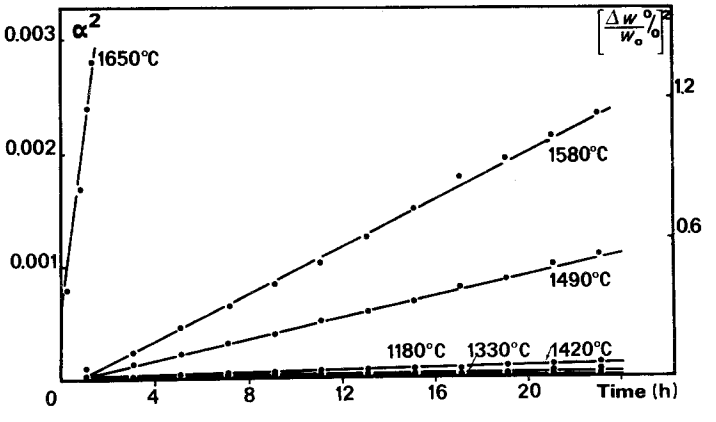

Figure 2 Parabolic plots of fractional weight gain of a specimen in air.

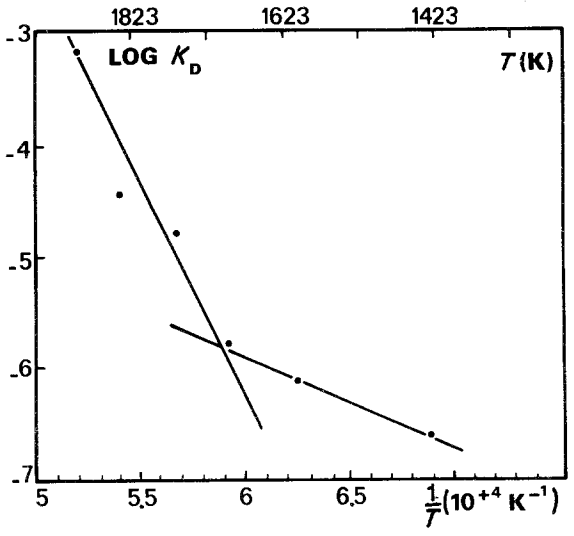

Figure 3 Arrhenius plot of parabolic rate constants for oxidation in air.

in air are due to the oxidation of the intergranular phase. A diffraction pattern (Fig. 4a) corresponding to a triple junction shows a set of spotted rings. Dark-field observations obtained by using a diffraction geometry set-up that avoids Bragg beams contribution through the objective aperture reveal a microcrystalline intergranular phase (Fig. 4b). During oxidation, the devitrification of the boundary phase is not complete.

The results of TEM investigation into the microstructure (absence of cavities or loosenings at grain boundaries) strongly suggest an ionic intergranular diffusion. Because of the compositional gradient between the surface and the interior of the sample, oxidation results from an inward diffusion of oxygen coupled with an outward diffusion of nitrogen. The diffusion of oxygen could be the limiting step.

3.2.2. 1420 to 1650° C interval

At high temperature, silicon nitride and silicon oxynitride contribute more to the overall weight gain.

SEM shows microstructural changes in the coating. At 1420° C, the oxide layer completely covers the specimen but converts at 1650° C into a glassy porous scale and the porosity begins at the internal interface. As has been pointed out for corrosion of nitrogen ceramics [6], metallic impurities which cannot be accommodated in the lattice of silicon nitride move to the surface. In order to determine if the morphology alterations of the scale are related to these compositional changes, X-ray microanalysis (EDAX) was used to follow the intergranular shift of yttrium. The resulting data show a yttrium depletion of the bulk coupled with an increase of the content at the internal interface (Fig. 5a and b). To obtain a significant change in the composition and thus, accurate results, we oxidized samples for extended times, but pores due to nitrogen release disrupted the oxide scale (Fig. 5c) and it is thus unsafe to conclude on the yttrium distribution type. Moreover, the internal interface is pitted (Fig. 5d) and as for

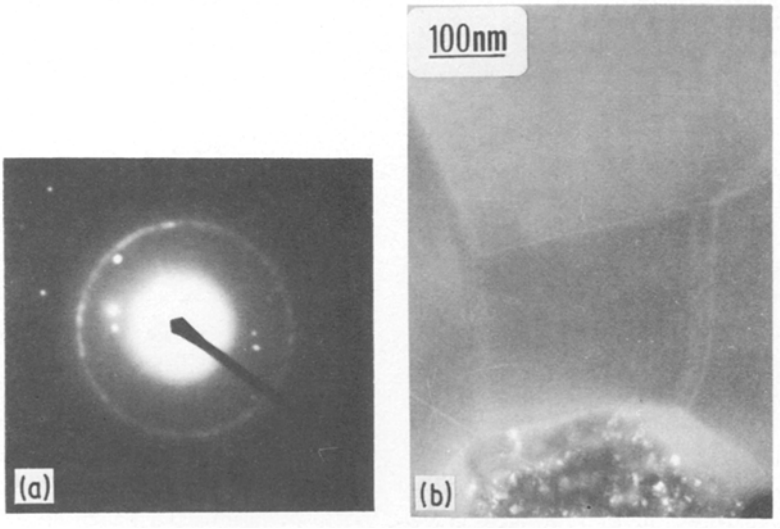

Figure 4 Transmission electron micrographs of an oxidized sample at 1400° C. (a) Diffraction pattern of a triple grain junction; (b) microprecipitates (dark field).

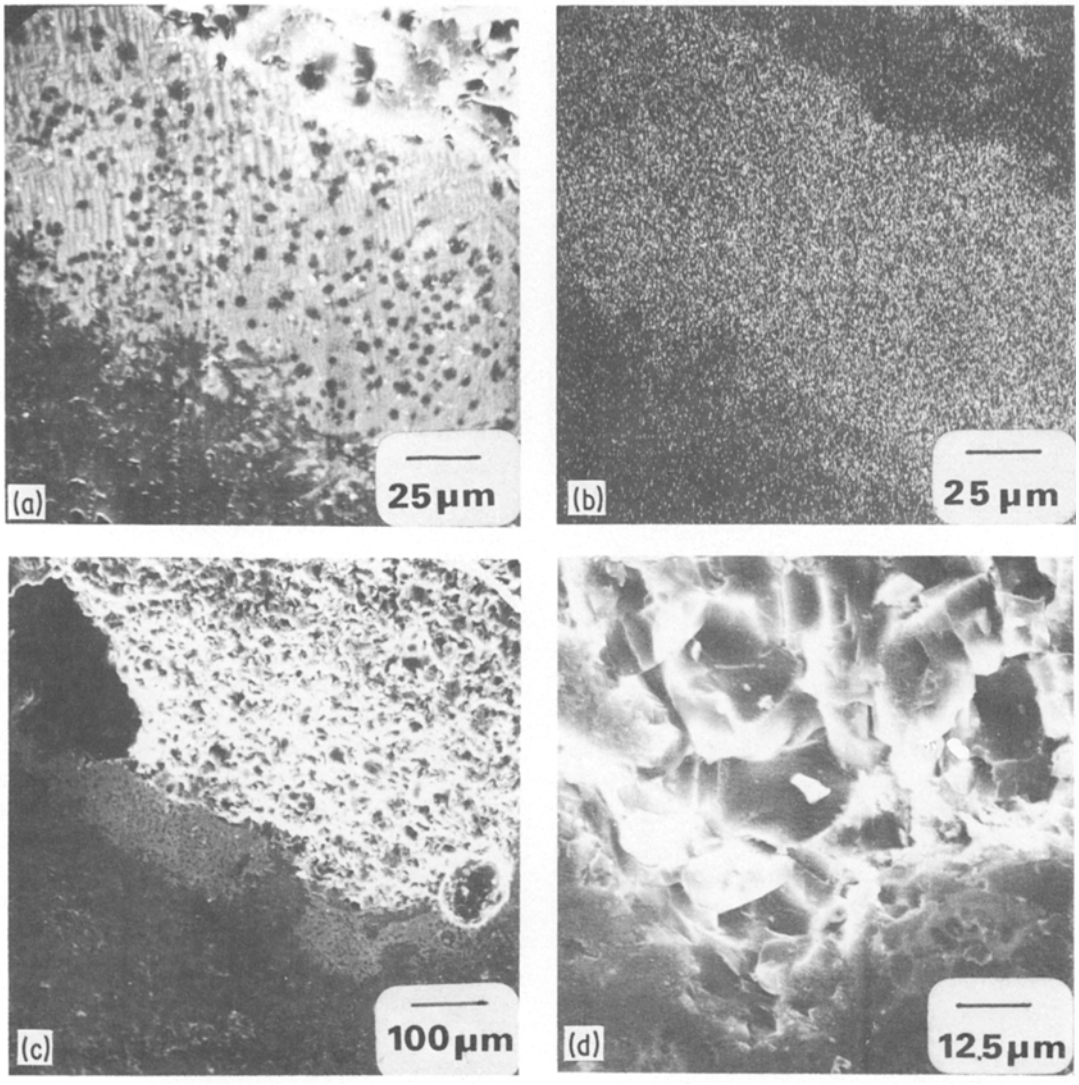

Figure 5 (a) Scanning electron micrograph of the oxide–nitride interface. (b) X-ray microanalysis of yttrium. (c) Scanning electron micrograph of a polished cross section of a sample, bulk–internal interface–oxide scale. (d) Grain boundary at the internal interface.

other alloys, oxidation induces a widening of grain boundaries. The above experimental results indicate that many reactions interact during oxidation. Therefore, it is difficult to suggest a quantitative interpretation of the mechanism [6] and to model the oxidation phenomena; so we shall restrict our objective to a discussion.

For kinetics at temperatures higher than 1420° C, as the viscosity of the grain boundary phase containing nitrogen diminishes, the mobility of diffusing species increases. At the start of the reaction, the oxidation of the nitrogen glassy phase produces an outward flux of yttrium and nitrogen. This high content of yttrium induces plasticity of the oxide layer which allows the release of gaseous nitrogen through its connected pore structure. As the scale is not protective, oxygen flows into the internal interface and oxidizes fresh surfaces of silicon nitride grains or the intergranular glass. The pore distribution is changed by nitrogen bubbling and the reaction continues. Furthermore, yttrium diffusion leads to a solution of silicon nitride along grain boundaries and especially at the internal interface where the yttrium concentration is high. This glass yields nitrogen which moves along the same path. When the steady state is established the sample is formed by three zones: the oxide scale,

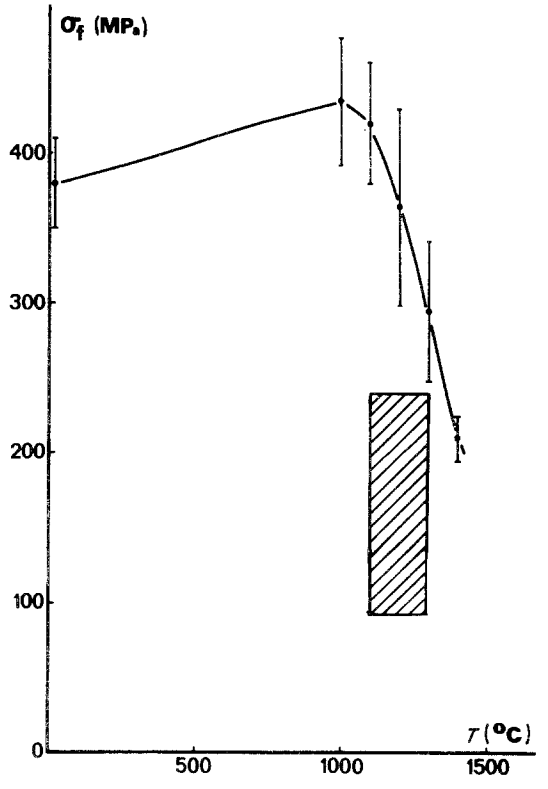

Figure 6 Three-point bending strength as a function of temperature. Bars correspond to a 90% interval of confidence on the mean value of the modulus of rupture. The dashed zone shows the conditions under which the creep experiments were performed.

the subscale at the internal interface, and the substrate. It proves that the nitrogen supply to the subscale at the internal interface is related to the yttrium flux, the moving species being a complex combination between yttrium and nitrogen. The diffusion of this "yttrium–nitrogen" compound species, which results from a compositional gradient in the glassy phase, should be the limiting step.

4. Creep

The results of the strength experiments are plotted in Fig. 6. Rupture occurs in a purely brittle way even at the higher temperature.

4.1. General behaviour

Representative curves of the creep behaviour are given in Fig. 7. A very long primary period was observed, in which the creep rate, after a rapid evolution for a few hours, diminished very slowly. This stage of slowly decreasing creep rate will be referred to as the "pseudo-stationary stage". Constant creep rates were measured only beyond 470 h during a test which lasted over 700 h (Fig. 8). No tertiary stage was observed.

It is now well established [7] that three concurrent mechanisms may be cited as responsible for the general behaviour of polyphase Si_3N_4 alloys: viscoelastic, diffusional and cavitational creep mechanisms. For the present alloy, the creep strain consists of only two components within the studied stress and temperature ranges: a viscoelastic component which is dominant during the first hours of the tests and a diffusional component which becomes the main source of deformation during the stationary stage.

4.2. Quantitative approach

The approach to obtain temperature dependence of the creep rate, $\dot{\varepsilon}$, and to characterize applied stress influence during steady-state is generally through the phenomenological relation:

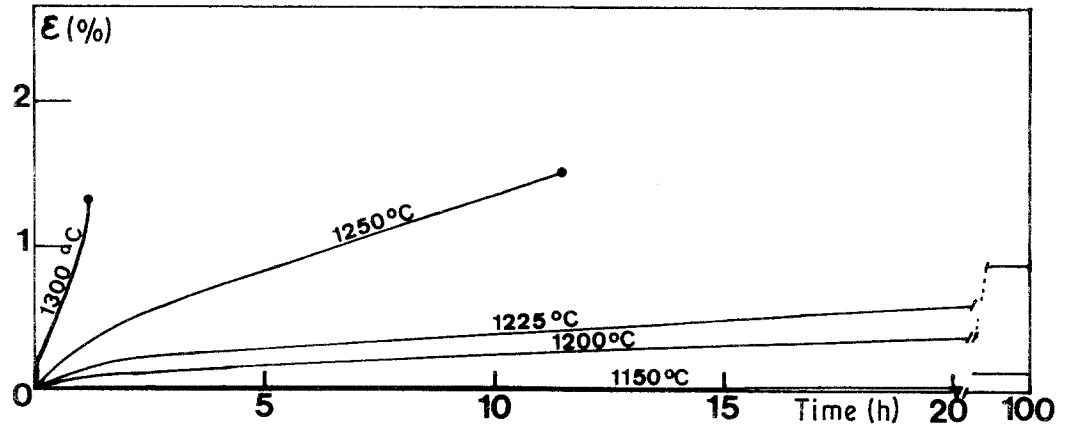

Figure 7 Creep curves at various temperatures at a stress of 240 MPa.

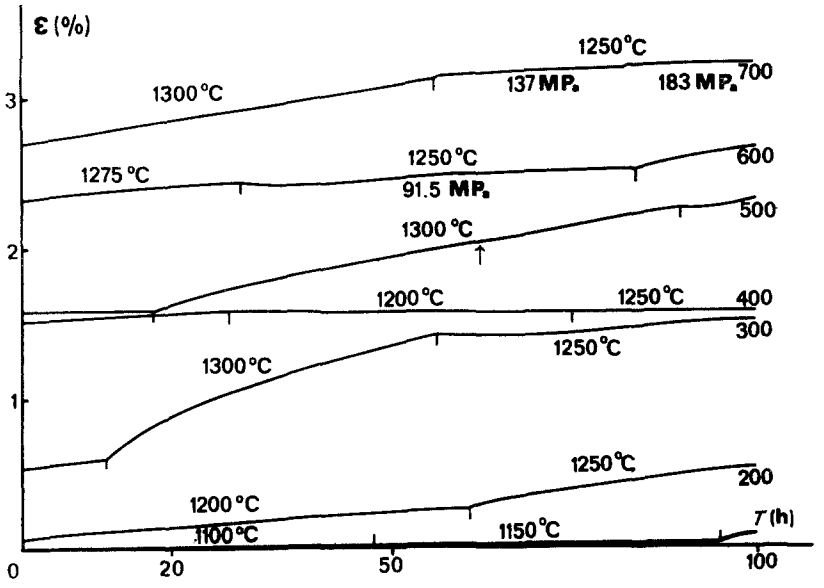

Figure 8 Creep curve of an as-sintered sample. Temperature steps at 91.5 MPa then stress steps at 1250° C. The arrow indicates the onset of the true stationary stage.

$$\dot{\epsilon} = f(S)\,\sigma^n \exp -(E/RT) \qquad (1)$$

where σ is the applied stress, n the stress exponent, E the activation energy, R the Boltzmann constant, T the absolute temperature, and $f(S)$ some function of the material and its structure.

Whereas under our experimental conditions, there is no grain growth in our material, the oxidizing atmosphere leads to an evolution of the microstructure (width of the glassy film at the grain boundaries) and of the composition of the glassy phase. Determinations of stress exponents (and respective activation energies) suppose that creep rates are measured for identical values of $f(S)$. In the present case, it seems reasonable to assume that similar compositions and structures are obtained for equally oxidized states. The results of oxidation kinetics (Fig. 2) allow us to relate the fractional weight gain (α), the time (in h) and the temperature (T) by the following equation in the temperature range investigated.

$$\alpha^2 = 0.13\,t \exp\,[-1.914 \times 10^4/T] \qquad (2)$$

Fig. 9 shows the plots of $\log \dot{\epsilon}$ against T^{-1} for different values of α corresponding to time within the pseudo-stationary stage. The three straight lines have the same slope from which an activation energy of 720 kJ mol^{-1} is derived. At 1200° C, for $t = 470$ h, the fractional weight gain is 1.5×10^{-2}, which corresponds to an oxidized depth of 1.7 mm, that is, a reaction virtually completed in 4 mm thick bars. For longer times, the microstructure is stabilized, the creep rate constant, the stress exponent equal to $n = 1$. The viscoelastic component of the strain is then negligible and the creep is diffusional. Nevertheless, the activation energy remains the same (curve 4 in Fig. 9).

4.3. Discussion

Arons and Tien [8] have shown that permanent creep and viscoelastic deformation are parallel reactions and can be treated independently. Lange *et al.* [7] came to the same conclusion. Hence, in the pseudostationary stage, the whole deformation is the sum of the viscoelastic component, ϵ_v, and of the diffusional component ϵ_d; i.e.

$$\epsilon = \epsilon_v + \epsilon_d \text{ and } \dot{\epsilon} = \dot{\epsilon}_v + \dot{\epsilon}_d \qquad (3)$$

During the steady-state creep, when the creep is purely diffusional, the stress fields which build up from the buttressing of two adjacent grains on ledges along the grain boundaries act as sources of differential chemical potentials required as the driving force for a solution precipitation mechanism with two steps acting in series: the transfer of atoms across the crystal–glass interface and the diffusional transport of matter through the glassy phase. If the limiting step is the transfer across the crystal–glass interface, the activation energy will be linked to the latent heat of solution of the Si_3N_4 crystal into the glass; if it is the matter

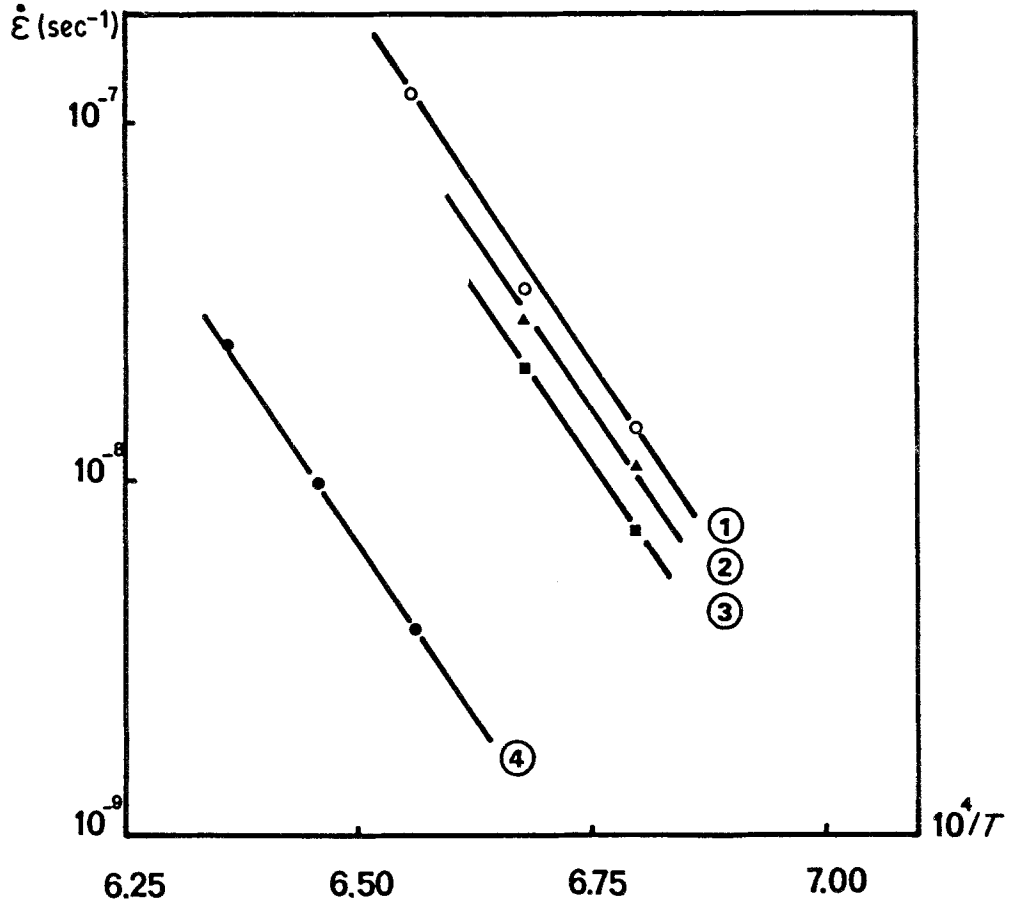

Figure 9 Apparent activation energies, determined at constant fractional weight gains, α, from the creep curves in Fig. 7: 1, $\alpha = 2.3 \times 10^{-3}$; 2, $\alpha = 3 \times 10^{-3}$; 3, $\alpha = 4.2 \times 10^{-3}$; and determined from Fig. 8 during the stationary stage: 4, $t > 470$ h.

transport through the glass which is the limiting step, then the activation energy will depend on the viscosity of the glassy phase [9].

According to the analysis of Lange *et al.* [10], the deformation strain for the viscoelastic component is:

$$\epsilon_v = \frac{\tau D^2}{EA}\left[1 - \exp - \frac{EAS_0}{D^3\eta}\, t\right] = \frac{\tau D^2}{EA}\left[1 - \exp - \frac{t}{\theta}\right] \quad (4)$$

where D is the mean-grain size, S_0 the thickness of the glassy interphase, A the areas of asperity, E the elastic modulus of the asperity, t the time, τ the shear stress at the grain boundary (which is related to the applied strain σ), η the glass viscosity and θ the relaxation time.

The deformation rate associated with this mechanism is:

$$\dot{\epsilon}_v = \frac{S_0}{\eta}\left[\frac{\tau}{D} - \frac{EA}{D^3}\,\epsilon_v\right] \quad (5)$$

During the pseudo-stationary stage, when the time is sufficiently long ($t > 5\theta$, that is about 10 h), $\dot{\epsilon}_v$ may be considered time independent and the creep rate has the form:

$$\dot{\epsilon}_v = \frac{1}{\eta} f(S_v, \sigma) \quad (6)$$

where S_v depends on the structural state of the material, $S_v(S_0, D, E, A)$.

From Equation 3, the creep rate may then be written:

$$\dot{\epsilon} = \dot{\epsilon}_v + \dot{\epsilon}_d = \frac{1}{\eta} f(S_v, \sigma) + S_d \sigma \exp(-E_d/RT) \quad (7)$$

where S_d depends on the structural state, and

E_d is the activation energy of the diffusional mechanism.

Supposing an Arrhenius law for the viscosity, which is valid if the temperature range is not too large [11], Equation 7 becomes:

$$\dot{\epsilon} = \frac{1}{\eta_0} f(S_v, \sigma) \exp\left(-\frac{E_v}{RT}\right) + S_d \sigma \exp\left(-\frac{E_d}{RT}\right)$$

where E_v is the activation energy of the glass viscosity.

The experimental results in Section 4.2 show that at constant fractional weight gains, the apparent activation energy is the same whatever the value of α, and is equal to the activation energy measured in the true stationary state. This may be possible only if $E_v = E_d$, that is if the viscosity of the glassy phase is rate controlling for the viscoelastic creep and for the diffusional creep. This leads us to conclude that the limiting step for the diffusional mechanism is the matter transport through the glassy phase and not the transfer of atoms across the crystal–glass interface.

In the case of silicon nitride hot-pressed with magnesia, Tsai and Raj [12] believe that it is the interface control case which applies. A comparison between their theoretically estimated creep rate and the experimental results of Lange *et al.* [7] bears this out. Babini *et al.* point out that the great difference in oxidation rates between Si_3N_4/MgO and Si_3N_4/Y_2O_3 is very likely linked to the different viscosities of the intergranular phase of each material. At the temperatures involved, a variation in viscosity of two orders of magnitude compares quite well with the differences in oxidation kinetics [13]. Matter transport in the glassy phase might be much more difficult in Si_3N_4/Y_2O_3 than in Si_3N_4/MgO and would become the limiting step. This result may be compared with the results drawn by Hampshire and Jack [14] from the study of the kinetics of sintering of Si_3N_4 using MgO and Y_2O_3 as additives. They have concluded that the rate controlling process is different in the two cases: solution into or precipitation from the liquid for Si_3N_4–MgO and diffusion through the liquid for Si_3N_4–Y_2O_3.

Finally, the activation energy for creep is close to the activation energy for oxidation in the higher temperature range where the reaction is controlled by the migration of a "yttrium–nitrogen" compound species through the intergranular phase. This suggests that it is the migration of the same species which is involved in the creep mechanism.

5. Conclusion

Oxidation kinetics of a SiYON alloy (Si_3N_4–Si_2N_2O–$Y_2Si_2O_7$ = 70–25–5 mol%) follow two different mechanisms. In the low temperature interval (1180 to 1420° C), experimental data and TEM observations suggest that the preferential oxidation of the nitrogen glass is governed by the inward diffusion of ionic oxygen. At higher temperatures, the fact that the formation of pores in the oxide scale originates in the release of nitrogen at the internal interface, proves that the oxidation of the nitrogen glass takes place in this zone. In addition, microanalysis data show a segregation of yttrium in this subscale. Thus, it seems that the diffusion in the intergranular phase to the internal interface of a "yttrium–nitrogen" compound species is the limiting step.

In the stress and temperature ranges investigated, this SiYON alloy does not exhibit significant cavitation. The creep deformation is the sum of a viscoelastic component and of a diffusional component.

The comparison of creep behaviour and oxidation resistance shows that a true stationary stage is reached when the oxidation reaction is achieved in the bulk of the samples. The activation energy for the viscoelastic and the diffusional components of the creep strain is the same. It is concluded that the limiting step for the diffusional mechanism is the transport of matter through the glassy grain boundary phase and that the diffusing species may be a "yttrium–nitrogen" compound as in the high temperature oxidation domain.

Acknowledgements

We wish to thank Dr P. Lortholary for electron microscopy and microanalysis assistance (service de Microscopie, Université de Limoges). This work was supported by the Centre National de la Recherche Scientifique under the ATP no. 0413.

References

1. D. R. CLARKE and G. THOMAS, *J. Amer. Ceram. Soc.* 60 (1977) 491.
2. B. S. B. KARUNARATNE and M. H. LEWIS, *J. Mater. Sci.* 15 (1980) 449.
3. G. E. GAZZA, *J. Amer. Ceram. Soc.* 56 (1973) 662.
4. F. F. LANGE, S. C. SINGHAL and R. C. KUZNICKI, *ibid.* 60 (1977) 249.
5. P. GOURSAT, C. DUMAZEAU and M. BILLY, Enivronmental Degradation of High Temperature Materials", Vol. 2 (Proc. Inst. Metal. Series, Chameleon Press, London, 1980) pp. 3/15.

6. S. C. SINGHAL and F. F. LANGE, *J. Amer. Ceram. Soc.* 60 (1977) 190.
7. F. F. LANGE, B. I. DAVIS and D. R. CLARKE, *J. Mater. Sci.* 15 (1980) 601.
8. R. M. ARONS and J. K. TIEN, *ibid.* 15 (1980) 2046.
9. R. RAJ and P. E. D. MORGAN, *J. Amer. Ceram. Soc.* 64 (1981) C143.
10. F. F. LANGE, D. R. CLARKE and B. J. DAVIS, *J. Mater. Sci.* 15 (1980) 611.
11. J. ZARZYCKI, "Les verres et l'état vitreux" (Masson, Paris, 1982).
12. R. J. TSAI and R. RAJ, *J. Amer. Ceram. Soc.* 65 (1982) C88.
13. G. N. BABINI, A. BELLOSI and P. VINCENZINI, in "Science of Ceramics 11", edited by R. Carlsson and S. Karlsson (Swedish Ceramic Society, 1981) p. 291.
14. S. HAMPSHIRE and K. H. JACK, "Special Ceramics", Vol. 7, edited by D. Taylor and P. Popper (British Ceramic Society, 1981) p. 37.

Received 18 November 1983
and accepted 26 July 1984